Quantum sensitivity limits of an optical magnetometer based on atomic phase coherence

Michael Fleischhauer* and Marlan O. Scully
Department of Physics, Texas A&M University, College Station, Texas 77843
and Max-Planck-Institut für Quantenoptik, 85742 Garching, Germany
(Received 1 March 1993; revised manuscript received 16 August 1993)

An optical magnetometer based on atomic coherence effects is analyzed using a quantum Langevin approach. The large dispersion of a phase-coherent atomic medium ("phaseonium") at a point of vanishing absorption is used to detect magnetic level shifts via optical phase measurements in a Mach-Zehnder interferometer with sensitivities potentially superior to state-of-the-art devices. Effects of Doppler broadening and fluctuations of the driving field are discussed and a comparison to standard optical-pumping magnetometers is made.

PACS number(s): 42.50.Lc, 07.60.Ly, 07.55.+x

I. INTRODUCTION

The development of SQUID (superconducting quantum interference device) magnetometers [1], based on quantum interference effects between supercurrents, opened a variety of fascinating applications in biology, medicine, and electrical engineering. With the advanced techniques of multiple SQUID arrays it is now possible, for instance, to study the tiny magnetic fields produced within the human brain with a field strength of less than 10^{-10} G.

Recently we have proposed an optical method to detect magnetic fields, based on quantum interference effects in atomic systems, which in principle provides sensitivities comparable to that of a SQUID without the need of cryogenic cooling [2]. In this paper we investigate the quantum noise limits of the sensitivity of such a device.

One way of detecting magnetic fields by optical means is to make use of the Zeeman effect [3]. The interaction of the magnetic moment of an atom with an external magnetic field leads to a perturbation of the energy levels. Associated with this is a shift of the atomic transition frequency.

$$\delta\omega_{ab} = aB \tag{1}$$

between the two levels a and b. Here $a=(\mu_B/\hbar)(m_a g_a - m_b g_b)$ contains Bohr's magneton, the magnetic quantum numbers, and the gyromagnetic factors and can be of the order of $10^7\ \mathrm{s}^{-1}/\mathrm{G}$. Although for magnetic fields of order 10^{-10} G this frequency shift is very tiny, it leads to a substantial change of the index of refraction at the atomic resonance

$$\delta n \propto \delta\omega_{ab} \ . \tag{2}$$

This variation causes a phase shift of a light beam transmitted through the medium, which then can be detected with very high accuracy by interferometric means. As can be seen from Fig. 1 for the case of a two-level atom, usual unsaturated materials are highly absorbing near the atomic resonance, which prevents an application of the high dispersion.

This absorption-dispersion relationship, however, changes completely if we consider atomic systems which display quantum coherence and interference effects [4–9]. In such systems, the absorption of a photon by an atom in the lower level can be canceled almost perfectly. This led to the prediction and observation of such effects as nonabsorbing resonances [4], lasing without population inversion [5–8], and the possibility of an ultralarge index of refraction in a completely transparent medium [9].

A typical spectrum of the linear susceptibility for a nonabsorbing resonance is shown in Fig. 2. At resonance ($\Delta=0$) we note a vanishing imaginary part of the susceptibility χ'', indicating a point of zero absorption. At the same time, the real part χ', which determines the index of refraction, displays a large slope. This gives the ingredients for the highly sensitive magnetometer proposed in Ref. [2]: A small magnetic field induces a variation in the index of refraction which causes a phase shift of a

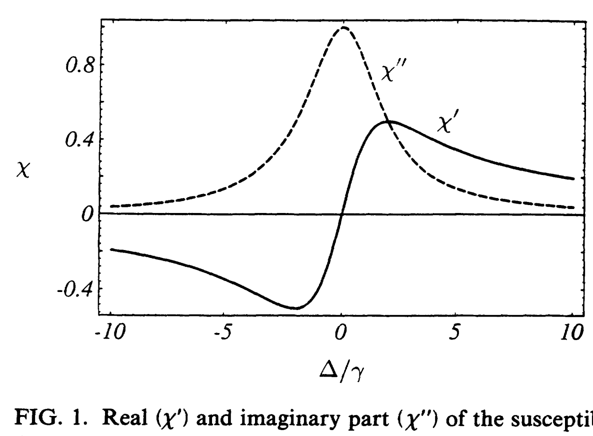

FIG. 1. Real (χ') and imaginary part (χ'') of the susceptibility (in arbitrary units) for a two-level atom in the ground state as a function of the atom-field detuning $\Delta=\omega_{ab}-\nu$. γ is the radiative decay rate. At resonance one recognizes a large slope of χ' indicating a large dispersion of the index of refraction. A small magnetic shift of the optical transition frequency leads to a change of the index of refraction for a probe field of fixed frequency ν.

---

*Permanent address: Ludwig-Maximilians-Universität, Sektion Physik, Theresienstraße 37, 80333 München, Germany.

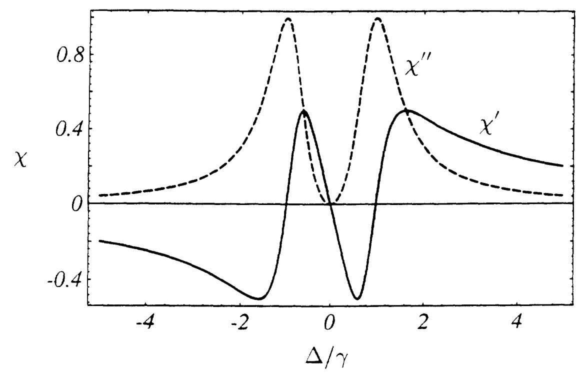

FIG. 2. Susceptibility spectrum of a nonabsorbing resonance. Displayed are the real (line) and imaginary parts (dashed) of the susceptibility in arbitrary units as a function of the atom-field detuning $\Delta=\omega_{ab}-\nu$.

transmitted probe field.

We here calculate the value of this phase shift for the particular atomic configuration shown in Fig. 3, in which a strong driving field between the unpopulated levels a and c creates electromagnetically induced transparency on the a-b transition [7]. We determine the quantum noise limits for the phase shift measurement in a Mach-Zehnder interferometer thereby taking into account effects of pump laser fluctuations, Doppler broadening, and thermal population of level c. To this end we analyze in Sec. II the response of the phase coherent medium on the probe field within a Langevin approach. In Sec. II A we calculate the linear susceptibility of the medium and in Sec. II B we evaluate the fluctuations imposed on the probe field by the atoms. The signal and noise in the actual setup of the Mach-Zehnder interferometer are then analyzed in Sec. III. In Secs. IV and V we discuss the influence of Doppler broadening and collisional pumping on the magnetometer operation. In Sec. VI we compare the sensitivity of our magnetometer to standard optical pumping magnetometer. A summary of the results is given in Sec. VII.

II. LANGEVIN APPROACH TO THE HIGH-INDEX MATERIAL

In this section we analyze the optical properties and the quantum noise of the atomic system shown in Fig. 3.

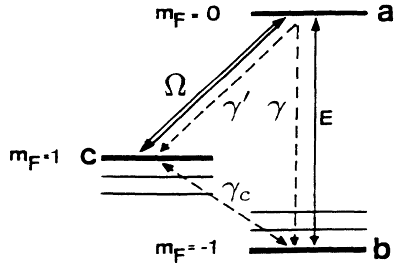

FIG. 3. A configuration in which strong driving field of Rabi frequency Ω couples levels a and c. Radiative decay from a to b and a to c goes at rates γ and γ' whereas collisional phase decay of the c-b polarization occurs at rate γ_c. The electric field of the probe laser is denoted by E.

A strong driving field of Rabi frequency Ω couples the upper level a of a dipole allowed optical transition a-b to an auxiliary level c inducing transparency on this transition. The interaction of the probe field $\hat{E}$ and the strong driving field with a single atom is described by the Hamiltonian

$$H^{\text{int}}=-\wp(\hat{E}^{(-)}\hat{\sigma}_0+\hat{E}^{(+)}\hat{\sigma}_0^\dagger)-\hbar(\Omega^*\hat{\sigma}_2+\Omega\hat{\sigma}_2^\dagger)\ , \tag{3}$$

where $\wp$ is the dipole moment of the $a\rightarrow b$ transition, $\hat{E}^{(+)}$ ($\hat{E}^{(-)}$) are the positive- (negative-) frequency part of the probe field strength, the atomic variables are defined as

$$\begin{aligned}\hat{\sigma}_0&=|b\rangle\langle a|\ ,\quad \hat{\sigma}_a=|a\rangle\langle a|\ ,\\ \hat{\sigma}_1&=|b\rangle\langle c|\ ,\quad \hat{\sigma}_b=|b\rangle\langle b|\ ,\\ \hat{\sigma}_2&=|c\rangle\langle a|\ ,\quad \hat{\sigma}_c=|c\rangle\langle c|\ ,\end{aligned} \tag{4}$$

and the strong driving field is described by the stochastic c-number variable Ω.

The equations of motion of the atomic variables can be obtained from the Hamiltonian Eq. (1). Including the decay processes indicated in Fig. 3, they read in the interaction picture

$$\dot{\hat{\sigma}}_a=-(\gamma+\gamma')\hat{\sigma}_a-i\frac{\wp}{\hbar}(\hat{E}^{(-)}\hat{\sigma}_0-\text{H.a.})-i(\Omega^*\hat{\sigma}_2-\text{H.a.})+\hat{F}_a\ , \tag{5a}$$

$$\dot{\hat{\sigma}}_b=\gamma\hat{\sigma}_a+i\frac{\wp}{\hbar}(\hat{E}^{(-)}\hat{\sigma}_0-\text{H.a.})+\hat{F}_b\ , \tag{5b}$$

$$\dot{\hat{\sigma}}_0=-[i\Delta+\tfrac{1}{2}(\gamma+\gamma')]\hat{\sigma}_0+i\frac{\wp}{\hbar}(\hat{\sigma}_b-\hat{\sigma}_a)\hat{E}^{(+)}+i\Omega\hat{\sigma}_1+\hat{F}_{\sigma_0}\ , \tag{5c}$$

$$\dot{\hat{\sigma}}_1=-[i(\Delta-\Delta')+\tfrac{1}{2}\gamma_c]\hat{\sigma}_1-i\frac{\wp}{\hbar}\hat{E}^{(+)}\hat{\sigma}_2^\dagger+i\Omega^*\hat{\sigma}_0+\hat{F}_{\sigma_1}\ , \tag{5d}$$

$$\dot{\hat{\sigma}}_2=-[i\Delta'+\tfrac{1}{2}(\gamma+\gamma'+\gamma_c)]\hat{\sigma}_2+i\frac{\wp}{\hbar}\hat{E}^{(+)}\hat{\sigma}_1^\dagger+i\Omega(\hat{\sigma}_c-\hat{\sigma}_a)+\hat{F}_{\sigma_2}\ , \tag{5e}$$

where $\Delta=\omega_{ab}-\nu$ and $\Delta'=\omega_{ac}-\nu'$; ν and ν' are the frequencies of the probe and driving field. Note that we have included in Eq. (5) a collision-induced perturbation of the energy of level c leading to a dephasing of the b-c and c-a polarizations, but have neglected collisional dephasing of the a-b polarization. This is a good approximation as long as the gas pressure is below 10 mTorr, corresponding to a density of $2\times10^{14}\ \text{cm}^{-3}$ at room temperature. The fluctuation operators $\hat{F}_x$ in Eqs. (5) have a zero mean value and are δ correlated,

$$\langle\hat{F}_x(t)\hat{F}_y(t')\rangle=\langle\hat{F}_x\hat{F}_y\rangle\delta(t-t')\ . \tag{6}$$

The diffusion coefficients $\langle\hat{F}_x\hat{F}_y\rangle$ have been calculated using the generalized fluctuation-dissipation theorem [10] and are listed in Appendix A.

Dalton and Knight [11] have shown that fluctuations of the pump laser field can essentially influence the optical properties of driven atomic systems. In our case the finite linewidth of the pump laser affects the effective lifetime of the c-b polarization. In order to make the effect of the finite pump-laser linewidth transparent, we transform the Langevin Eq. (5) to new variables:

$$\Omega=\Omega_0 e^{i\phi}\ ,\quad \hat{\sigma}_2=\hat{\sigma}_{20}e^{i\phi}\ ,\quad \hat{\sigma}_1=\hat{\sigma}_{10}e^{-i\phi}\ , \tag{7}$$

where we have separated the phase ϕ of the pump laser.

We will show in Appendix B that, under conditions typical for the magnetometer discussed here, a depletion of the pump field due to the interaction with the coherent medium can be disregarded. Therefore Ω_0 as well as ϕ can be viewed on as the amplitude and phase of the unperturbed pump laser. The phase in an ordinary laser undergoes free diffusion, which means it obeys an equation of motion [10,12]

$$\dot{\phi}(t)=\mu(t)\ , \tag{8}$$

where $\mu(t)$ is a δ-correlated Langevin-noise operator, whose diffusion coefficient is given by the pump-laser linewidth γ_L:

$$\langle \mu(t)\mu(t')\rangle=\gamma_L\delta(t-t')\ . \tag{9}$$

We thus have in the new variables

$$\dot{\hat{\sigma}}_{10}=-[i(\Delta-\Delta')+\tfrac{1}{2}\gamma_c-i\mu(t)]\hat{\sigma}_{10} -i\frac{\wp}{\hbar}\hat{E}^{(+)}\hat{\sigma}^*_{20}+i\Omega_0\hat{\sigma}_0+\tilde{F}_{\sigma_{10}}\ , \tag{10a}$$

$$\dot{\hat{\sigma}}_{20}=-[i\Delta'+\tfrac{1}{2}(\gamma+\gamma'+\gamma_c)+i\mu(t)]\hat{\sigma}_{20} +i\frac{\wp}{\hbar}\hat{E}^{(+)}\hat{\sigma}^*_{10}+i\Omega_0(\hat{\sigma}_c-\hat{\sigma}_a)+\tilde{F}_{\sigma_{20}}\ , \tag{10b}$$

with $\tilde{F}_{\sigma_{10}}=\hat{F}_{\sigma_1}e^{-i\phi}$ and $\tilde{F}_{\sigma_{20}}=\hat{F}_{\sigma_2}e^{i\phi}$.

A. Semiclassical steady-state solutions and susceptibilities

In a first step we calculate the linear susceptibility of the coherent medium with respect to the probe field, assuming a small probe field strength $\hat{E}$. We derive expressions for the mean values of the populations $\langle\hat{\sigma}_a\rangle$, $\langle\hat{\sigma}_b\rangle$, and $\langle\hat{\sigma}_c\rangle$ and of the polarization $\langle\hat{\sigma}_{20}\rangle$ in zeroth order of the probe field, and for the mean values of the polarizations $\langle\hat{\sigma}_0\rangle$ and $\langle\hat{\sigma}_{10}\rangle$ in first order of the probe field. We thereby replace the probe-field strength $\hat{E}(z,t)$ and the Rabi frequency of the driving field $\Omega_0(t)$ by their semiclassical steady-state values $\overline{E}(z)$ and $\overline{\Omega}_0$.

From Eqs. (5) and (10) we find the semiclassical set of equations in zeroth order of E

$$\langle\dot{\hat{\sigma}}_a^{(0)}\rangle=-(\gamma+\gamma')\langle\hat{\sigma}_a^{(0)}\rangle-i\overline{\Omega}_0(\langle\hat{\sigma}_{20}^{(0)}\rangle-\text{c.c.})\ , \tag{11a}$$

$$\langle\dot{\hat{\sigma}}_b^{(0)}\rangle=\gamma\langle\hat{\sigma}_a^{(0)}\rangle\ , \tag{11b}$$

$$\langle\dot{\hat{\sigma}}_{20}^{(0)}\rangle=-[i\Delta'+\tfrac{1}{2}(\gamma+\gamma'+\gamma_c)]\langle\hat{\sigma}_{20}^{(0)}\rangle -i\langle\mu(t)\hat{\sigma}_{20}^{(0)}(t)\rangle+i\overline{\Omega}_0(\langle\hat{\sigma}_c^{(0)}\rangle-\langle\hat{\sigma}_a^{(0)}\rangle)\ , \tag{11c}$$

and in first order

$$\langle\dot{\hat{\sigma}}_0^{(1)}\rangle=-[i\Delta+\tfrac{1}{2}(\gamma+\gamma')]\langle\hat{\sigma}_0^{(1)}\rangle +i\frac{\wp}{\hbar}\overline{E}^{(+)}(\langle\hat{\sigma}_b^{(0)}\rangle-\langle\hat{\sigma}_a^{(0)}\rangle)+i\overline{\Omega}_0\langle\hat{\sigma}_{10}^{(1)}\rangle\ , \tag{12a}$$

$$\langle\dot{\hat{\sigma}}_{10}^{(1)}\rangle=-[i(\Delta-\Delta')+\tfrac{1}{2}\gamma_c]\langle\hat{\sigma}_{10}^{(1)}\rangle +i\langle\mu(t)\hat{\sigma}_{10}^{(0)}(t)\rangle-i\frac{\wp}{\hbar}\hat{E}^{(+)}\langle\hat{\sigma}_{20}^{\dagger(0)}\rangle +i\overline{\Omega}_0\langle\hat{\sigma}_0^{(1)}\rangle\ . \tag{12b}$$

The second terms on the right-hand side of Eq. (11c) and (12b) can be obtained by a formal integration of Eq. (10). We obtain

$$i\langle\mu(t)\hat{\sigma}_{10}(t)\rangle=-\int_0^t dt'\langle\mu(t)\mu(t')\hat{\sigma}_{10}(t')\rangle \simeq-\int_0^t dt'\langle\mu(t)\mu(t')\rangle\langle\hat{\sigma}_{10}(t')\rangle\ . \tag{13a}$$

Substituting the correlation function of the noise operator with the help of Eq. (9) we find

$$\begin{aligned} i\langle\mu(t)\hat{\sigma}_{10}(t)\rangle&=-\tfrac{1}{2}\gamma_L\langle\hat{\sigma}_{10}(t)\rangle\ ,\\ -i\langle\mu(t)\hat{\sigma}_{20}(t)\rangle&=-\tfrac{1}{2}\gamma_L\langle\hat{\sigma}_{20}(t)\rangle\ . \end{aligned} \tag{13b}$$

We then solve Eqs. (11) in steady state and obtain

$$\langle\hat{\sigma}_1^{(0)}\rangle=\langle\hat{\sigma}_c^{(0)}\rangle=\langle\hat{\sigma}_{20}^{(0)}\rangle=0\ , \tag{14a}$$

$$\langle\hat{\sigma}_b^{(0)}\rangle=1\ . \tag{14b}$$

Similarly we find from Eqs. (12)

$$\langle\hat{\sigma}_0^{(1)}\rangle=i\frac{\wp}{\hbar}\overline{E}^{(+)}\frac{i(\Delta-\Delta')+\frac{1}{2}\Gamma_c}{[\overline{\Omega}_0^2+\frac{1}{4}\Gamma_c(\gamma+\gamma')-\Delta(\Delta-\Delta')]^2+\frac{1}{4}[(\Delta-\Delta')(\gamma+\gamma')+\Delta\Gamma_c]^2} \times\left[\overline{\Omega}_0^2+\tfrac{1}{4}\Gamma_c(\gamma+\gamma')-\Delta(\Delta-\Delta')-\frac{i}{2}[(\Delta-\Delta')(\gamma+\gamma')+\Delta\Gamma_c]\right]\ , \tag{14c}$$

where $\Gamma_c=\gamma_c+\gamma_L$. The linear optical properties of the medium are determined by the susceptibility [10] defined as

$$\chi\equiv\frac{P^{(1)}}{\epsilon_0\overline{E}^{(+)}}=\frac{\wp N\langle\sigma_0^{(1)}\rangle}{\epsilon_0\overline{E}^{(+)}}\ , \tag{15}$$

where N is the number density of atoms. For a measurement of very small magnetic fields we have $\Delta,\Delta'\ll\gamma$. Furthermore, we assume a sufficiently strong driving field such that $\overline{\Omega}_0^2\gg(\gamma+\gamma')\Gamma_c$ with $\Gamma_c\ll\gamma,\gamma'$. In this case we obtain from Eq. (14c) for the real and imaginary parts of the susceptibility, χ' and χ'', determining the dispersion and absorption of the medium:

$$\chi' \approx -\frac{\wp^2 N}{\hbar\epsilon_0}\frac{(\Delta-\Delta')}{\bar{\Omega}_0^2}\,, \tag{16a}$$

$$\chi'' \approx \frac{\wp^2 N}{\hbar\epsilon_0}\frac{\Gamma_c}{2\bar{\Omega}_0^2}\,. \tag{16b}$$

We note from Eq. (16b) that in the limit $\Gamma_c \to 0$ there is no absorption of the medium, although all population is in the lower level of the probe field transition. At the same time we recognize from Eq. (16a) that the index of refraction is linear in the detuning $\Delta-\Delta'$. Substituting $\wp$ by the radiative decay rate [10] $\gamma=\wp^2\nu^3/6\pi\hbar\epsilon_0 c^3$, we find for the index of refraction $n\approx 1+\frac{1}{2}\chi'$:

$$n \approx 1-\frac{3}{8\pi^2}\frac{\gamma}{\bar{\Omega}_0^2}\lambda^3 N(\Delta-\Delta')\,, \tag{17}$$

where λ is the wavelength of the atomic transition. Throughout this section we assume that the driving and the probe field are in resonance with the corresponding transitions in the absence of a magnetic field. As indicated in Fig. 3 the probe as well as the driving transition are sensitive to magnetic fields. Therefore in the presence of a magnetic field B parallel to the propagation direction of the two light fields we have [3]

$$\Delta=\frac{\mu_B}{\hbar}g_b B\,, \tag{18a}$$

$$\Delta'=-\frac{\mu_B}{\hbar}g_c B\,, \tag{18b}$$

where μ_B is Bohr's magneton and g_b and g_c are the gyromagnetic factors of levels b and c. A probe field propagating a distance L through the coherent medium with the index of refraction n given in Eq. (17) will acquire a relative phase shift

$$\Delta\phi_{\rm sig}=\frac{2\pi(n-1)L}{\lambda}=-\frac{3}{4\pi}\lambda^2 NL\frac{\gamma}{\bar{\Omega}_0^2}aB \tag{19a}$$

due to the magnetic field. The residual absorption of the coherent medium due to collisional dephasing of the b-c coherence and the finite linewidth of the driving laser leads to a reduction of the amplitude of the transmitted field by a factor κ,

$$\kappa=\exp\left\{-\frac{\pi}{\lambda}\chi'' L\right\}=\exp\left\{-\frac{3}{8\pi}\lambda^2 LN\frac{\gamma\Gamma_c}{\bar{\Omega}_0^2}\right\}. \tag{19b}$$

In the second part of Eq. (19b) we have inserted χ'' from Eq. (16b) and have again substituted $\wp$ in terms of γ. Hence the steady-state value of the probe field at the output of the gas cell is given by

$$\bar{E}^{(+)}(L)=\bar{E}^{(+)}(0)\kappa e^{i\Delta\phi_{\rm sig}}\,. \tag{20}$$

B. Noise properties

In order to determine the noise properties of the probe field at the output of the phaseonium gas cell we first analyze the quantum properties of the polarization of the medium at the operation point $\Delta=\Delta'=0$ (no magnetic field). To this end we apply a c-number Langevin approach (Fokker-Planck approach) [12,13]. In this approach correlation functions of the c-number variables correspond to normally ordered correlation functions of the original operators, where normal ordering is defined as

$$\hat{E}^{(-)},\hat{\sigma}_2^\dagger,\hat{\sigma}_1^\dagger,\hat{\sigma}_0^\dagger,\hat{\sigma}_a,\hat{\sigma}_b,\hat{\sigma}_c,\hat{\sigma}_0,\hat{\sigma}_1,\hat{\sigma}_2,\hat{E}^{(+)}\,. \tag{21}$$

The c-number Langevin equations can be obtained from the operator Eqs. (5) and (10) simply by replacing the operators by their c-number counterparts. The diffusion coefficients of the c-number Langevin operators $\mathcal{F}_x$ can be derived from the quantum diffusion coefficients as outlined in Appendix A. We have

$$\dot{\sigma}_a=-(\gamma+\gamma')\sigma_a-i\frac{\wp}{\hbar}(E^{(-)}\sigma_0-\text{c.c.})-i(\bar{\Omega}_0\sigma_{20}-\text{c.c.})+\mathcal{F}_a\,, \tag{22a}$$

$$\dot{\sigma}_b=\gamma\sigma_a+i\frac{\wp}{\hbar}(E^{(-)}\sigma_0-\text{c.c.})+\mathcal{F}_b\,, \tag{22b}$$

$$\dot{\sigma}_0=-[i\Delta+\tfrac{1}{2}(\gamma+\gamma')]\sigma_0+i\frac{\wp}{\hbar}(\sigma_b-\sigma_a)E^{(+)}+i\bar{\Omega}_0\sigma_{10}+\mathcal{F}_{\sigma_0}\,, \tag{22c}$$

$$\dot{\sigma}_{10}=-[i(\Delta-\Delta')+\tfrac{1}{2}\Gamma_c]\sigma_{10}-i\frac{\wp}{\hbar}E^{(+)}\sigma_{20}^*+i\bar{\Omega}_0\sigma_0+\mathcal{F}_{\sigma_{10}}\,, \tag{22d}$$

$$\dot{\sigma}_{20}=-(i\Delta'+\tfrac{1}{2}\Gamma)\sigma_{20}+i\frac{\wp}{\hbar}E^{(+)}\sigma_{10}^*+i\bar{\Omega}_0(\sigma_c-\sigma_a)+\mathcal{F}_{\sigma_{20}}\,, \tag{22e}$$

where $\mathcal{F}_{\sigma_{10}}=\tilde{\mathcal{F}}_{\sigma_{10}}+i\sigma_{10}(t_+)\mu(t)$, $\mathcal{F}_{\sigma_{20}}=\tilde{\mathcal{F}}_{\sigma_{20}}-i\sigma_{20}(t_+)\mu(t)$, and $\Gamma=\gamma+\gamma'+\gamma_c+\gamma_L$.

We now assume that the probe field is quasistationary, which means that the medium adiabatically follows the time evolution of the field. In this case we can neglect the time derivatives on the left-hand side of Eqs. (22), and obtain for the microscopic (dimensionless) polarization of the medium in first order of E:

$$\sigma_0^{(1)}(t)=i\frac{\wp}{\hbar}E^{(+)}\frac{\Gamma_c}{2[\bar{\Omega}_0^2+\frac{1}{4}(\gamma+\gamma')\Gamma_c]}+\mathcal{F}_p(t)\,, \tag{23}$$

where the effective Langevin noise operator $\mathcal{F}_p(t)$ is given by

$$\mathcal{F}_p(t)=\frac{1}{D}\left\{i\bar{\Omega}_0\mathcal{F}_{\sigma_{10}}+\frac{1}{2}\Gamma_c\mathcal{F}_{\sigma_0}+\frac{2\wp E^{(+)}\bar{\Omega}_0}{\hbar\Gamma}\mathcal{F}_{\sigma_{20}}^*+i\frac{\wp}{\hbar}E^{(+)}\left[\frac{1}{2}\left[1+\frac{\Gamma\Gamma_c}{4\bar{\Omega}_0^2}\right]\mathcal{F}_a-i\frac{\bar{\Omega}_0}{\Gamma}\left[1+\frac{\Gamma\Gamma_c}{4\bar{\Omega}_0^2}\right](\mathcal{F}_{\sigma_{20}}-\mathcal{F}_{\sigma_{20}}^*)+\left[\frac{\gamma+\gamma'}{2\gamma}+\frac{3\Gamma_c}{2\gamma}+\frac{\Gamma\Gamma_c(\gamma+\gamma')}{8\bar{\Omega}_0^2\gamma}\right]\mathcal{F}_b\right]\right\} \tag{24}$$

and

$$D=\bar{\Omega}_0^2+\frac{(\gamma+\gamma')\Gamma_c}{4}\ . \qquad (25)$$

The diffusion coefficients of $\mathcal{F}_p(t)$ can be determined from the atomic diffusion coefficients given in Appendix A. Restricting the calculation to the lowest-order contributions in the probe field E we find

$$\langle \mathcal{F}_p^*(t)\mathcal{F}_p(t')\rangle=\langle \mathcal{F}_p^*\mathcal{F}_p\rangle\delta(t-t') = \frac{\wp^2\Gamma_c}{\hbar^2\bar{\Omega}_0^4}\frac{(\gamma+\gamma')}{\gamma}\langle E^{(-)}(t)E^{(+)}(t)\rangle \times\delta(t-t') \qquad (26a)$$

and

$$\langle \mathcal{F}_p(t)\mathcal{F}_p(t')\rangle=-\frac{\wp^2\Gamma_c}{\hbar^2\bar{\Omega}_0^4}\langle E^{(+)}(t)E^{(+)}(t)\rangle\delta(t-t')\ , \qquad (26b)$$

where we have used again that Γ_c is small compared to γ, γ', and $\bar{\Omega}_0^2 \gg \gamma\Gamma_c$.

The equation of motion for the propagation of the slowly varying amplitude of the probe field reads [10]

$$\left[\frac{\partial}{\partial t}+c\frac{\partial}{\partial z}\right]E^{(+)}(z,t)=\frac{i\nu}{2\epsilon_0}P^{(1)}(z,t)\ , \qquad (27)$$

where we have introduced the macroscopic polarization

$$P(z,t)=\bar{P}(z,t)+\mathcal{F}_P(z,t) \qquad (28)$$

of the medium, which is determined by the atomic polarization σ_0. Its semiclassical value $\bar{P}$ reads

$$\bar{P}(z,t)=\wp N\bar{\sigma}_0(t)|_{E=\bar{E}(z)}\ , \qquad (29)$$

where N is the number density of atoms in the sample and $\bar{\sigma}_0$ is the semiclassical value of the microscopic polarization. As shown in Appendix C the Langevin noise operator $\mathcal{F}_P(z,t)$ is δ correlated and its diffusion coefficient is given by the diffusion coefficient of $\mathcal{F}_p(t)$;

$$\langle \mathcal{F}_P^{(*)}(z,t)\mathcal{F}_P(z',t')\rangle=\frac{\wp^2}{A}N\langle \mathcal{F}_p^{(*)}\mathcal{F}_p\rangle\delta(t-t')\delta(z-z')\ . \qquad (30)$$

We proceed by assuming small field fluctuations around the semiclassical steady-state values such that

$$E^{(\pm)}(z,t)=\bar{E}^{(\pm)}(z)+\delta E^{(\pm)}(z,t)\ . \qquad (31)$$

The correspondingly linearized propagation equation reads

$$\left[\frac{\partial}{\partial t}+c\frac{\partial}{\partial z}\right]\delta E^{(+)}(z,t)=\frac{i\nu}{2\epsilon_0}\delta P^{(1)}(z,t)\ , \qquad (32a)$$

where according to Eqs. (28) and (29)

$$\delta P(z,t)=i\frac{\wp^2 N}{\hbar}\frac{\Gamma_c}{2[\bar{\Omega}_0^2+\frac{1}{4}(\gamma+\gamma')\Gamma_c]}\delta E^{(+)}(z,t) +\mathcal{F}_P(z,t)\ . \qquad (32b)$$

Inserting Eq. (32b) into (32a) and performing a Fourier transformation yields the simple linear differential equation

$$c\frac{d}{dz}\delta E^{(+)}(z;\omega)=(i\omega-\eta c)\delta E^{(+)}(z;\omega)+\frac{i\nu}{2\epsilon_0}\mathcal{F}_P(z;\omega)\ , \qquad (33a)$$

where

$$\eta=\frac{\nu\chi''}{2c}=\frac{\nu\wp^2N}{2c\hbar\epsilon_0}\frac{\Gamma_c}{2[\bar{\Omega}_0^2+\frac{1}{4}(\gamma+\gamma')\Gamma_c]}\ . \qquad (33b)$$

Note that $e^{-\eta L}=\kappa$. We can easily integrate Eq. (33a) and obtain

$$\delta E^{(+)}(L;\omega)=\delta E^{(+)}(0;\omega)e^{i\omega(L/c)}e^{-\eta L} +\frac{i\nu}{2\epsilon_0 c}\int_0^L dz\, e^{-\eta(L-z)}e^{i(\omega/c)(L-z)} \times\mathcal{F}_P(z;\omega)\ . \qquad (34)$$

With Eq. (30) we eventually find for the correlation of the field fluctuations at the output of the phaseonium gas cell

$$\langle \delta E^{(+)}(L,t)\delta E^{(+)}(L,t')\rangle=\left\langle \delta E^{(+)}\left[0,t-\frac{L}{c}\right]\delta E^{(+)}\left[0,t'-\frac{L}{c}\right]\right\rangle e^{-2\eta L} -\frac{\wp^2\nu^2}{4\epsilon_0^2Ac^2}N\int_0^L dz\, e^{-2\eta(L-z)}\langle \mathcal{F}_p\mathcal{F}_p\rangle\Big|_{E=\bar{E}(z)}\delta(t-t') \qquad (35)$$

and

$$\langle \delta E^{(-)}(L,t)\delta E^{(+)}(L,t')\rangle=\left\langle \delta E^{(-)}\left[0,t-\frac{L}{c}\right]\delta E^{(+)}\left[0,t'-\frac{L}{c}\right]\right\rangle e^{-2\eta L} +\frac{\wp^2\nu^2}{4\epsilon_0^2Ac^2}N\int_0^L dz\, e^{-2\eta(L-z)}\langle \mathcal{F}_p^*\mathcal{F}_p\rangle\Big|_{E=\bar{E}(z)}\delta(t-t')\ . \qquad (36)$$

Substituting the diffusion coefficients Eq. (26) and making use of the initial condition $\delta E^{(\pm)}(0,t)=0$, we finally obtain for the field fluctuations at the output

$$\langle \delta E^{(+)}(L,t)\delta E^{(+)}(L,t')\rangle = \frac{\wp^4\nu^2 NL\Gamma_c}{4\hbar^2\epsilon_0^2 A\,\overline{\Omega}_0^4 c^2}\kappa^2\overline{E}^{(+)}(0)\overline{E}^{(+)}(0)\delta(t-t') , \quad (37a)$$

$$\langle \delta E^{(-)}(L,t)\delta E^{(+)}(L,t')\rangle = \frac{\wp^4\nu^2 NL\Gamma_c}{4\hbar^2\epsilon_0^2 A\,\overline{\Omega}_0^4 c^2}\frac{\gamma+\gamma'}{\gamma}\kappa^2\overline{E}^{(-)}(0)\overline{E}^{(+)}(0)\delta(t-t') . \quad (37b)$$

III. QUANTUM LIMITS OF MAGNETOMETER SENSITIVITY

To analyze the quantum limits of the magnetometer sensitivity we now calculate the signal and noise of the phase measurement in a Mach-Zehnder interferometer as shown in Fig. 4. Our measurement signal $\hat{j}$ is the difference of the photocounts of the two interferometer outputs. The balancing of the two outputs eliminates noise contributions from classical intensity fluctuations of the input probe field [14,15]. We assume here that both detectors have an efficiency of unity and that all beam splitter are lossless and have a 50% transmittivity.

Denoting the field strength at the Mach-Zehnder outputs by $\hat{E}_5$ and $\hat{E}_4$, we have

$$\hat{j}=\frac{2\epsilon_0 Ac}{\hbar\nu}\int_0^{t_m} d\tau[\hat{E}_5^{(-)}(\tau)\hat{E}_5^{(+)}(\tau)-\hat{E}_4^{(-)}(\tau)\hat{E}_4^{(+)}(\tau)] , \quad (38)$$

where A is the effective beam cross section and t_m is the measurement time. The values of the field strength in the different parts of the Mach-Zehnder interferometer, as indicated in Fig. 4, are related by the beam-splitter input-output relations

$$\hat{E}_5^{(\pm)}=\pm\frac{i}{\sqrt{2}}\hat{E}_3^{(\pm)}+\frac{1}{\sqrt{2}}\hat{E}_2^{(\pm)} , \quad (39a)$$

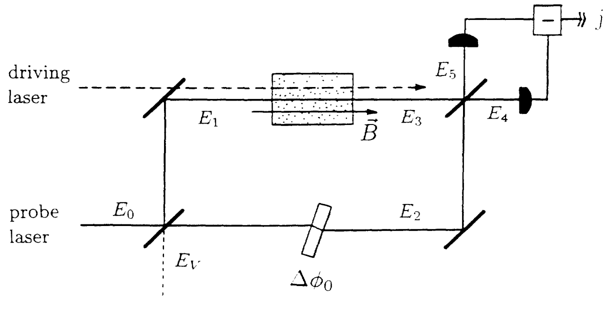

FIG. 4. Mach-Zehnder interferometer. Probe laser radiation acquires a magnetic-field-dependent phase shift (relative to $\Delta\phi_0$) which is detected by a difference measurement of the two outputs.

$$\hat{E}_4^{(\pm)}=\frac{1}{\sqrt{2}}\hat{E}_3^{(\pm)}\pm\frac{i}{\sqrt{2}}\hat{E}_2^{(\pm)} , \quad (39b)$$

and

$$\hat{E}_2^{(\pm)}=\left[\frac{1}{\sqrt{2}}\hat{E}_0^{(\pm)}\pm\frac{i}{\sqrt{2}}\hat{E}_v^{(\pm)}\right]e^{\pm i\Delta\phi_0} , \quad (39c)$$

$$\hat{E}_1^{(\pm)}=\pm\frac{i}{\sqrt{2}}\hat{E}_0^{(\pm)}+\frac{1}{\sqrt{2}}\hat{E}_v^{(\pm)} , \quad (39d)$$

where $\hat{E}_v$ is the vacuum-field contribution from the unused input port.

To determine the mean output signal $\langle\hat{j}\rangle$ and the principle measurement error $\langle\Delta\hat{j}^2\rangle$, we again make use of the c-number approach introduced in Sec. II. $\langle\hat{j}\rangle$ and $\langle\Delta\hat{j}^2\rangle$ can be expressed in terms of a corresponding c-number variable j via

$$\langle\hat{j}\rangle=\langle j\rangle , \quad (40a)$$

$$\langle\Delta\hat{j}^2\rangle=\langle\Delta j^2\rangle+\frac{1+\kappa^2}{2}\langle n_{\rm in}\rangle . \quad (40b)$$

Here

$$n_{\rm in}=\frac{2\epsilon_0 Act_m}{\hbar\nu}\langle\hat{E}_0^{(-)}\hat{E}_0^{(+)}\rangle \quad (41)$$

is the number of input photons passing through the interferometer during the measurement time. It can be expressed in terms of the input power $P_{\rm in}$ as $n_{\rm in}=(P_{\rm in}t_m)/\hbar\nu$. The first term of Eq. (40b) results from fluctuations due to the interaction of the probe field with the coherent atomic medium. The second term describes shot noise. It originates from the vacuum fluctuations of the radiation field. A brief derivation of this term is given in Appendix D.

In the c-number approach, the field operators in Eqs. (39) are replaced by the corresponding c-number variables and the vacuum contribution E_v vanishes.

In the first step of our calculation we derive an expression for the mean output signal $\langle j\rangle$, which is determined by the semiclassical field value at the output of the phaseonium gas cell, Eq. (20). with the help of the beam-splitter relations, Eq. (39), we obtain

$$\langle\hat{j}\rangle=n_{\rm in}\kappa\cos(\Delta\phi_{\rm sig}-\Delta\phi_0) , \quad (42)$$

where $\Delta\phi_0$ is the phase shift due to a phase plate in the other arm of the interferometer. Adjusting the parameters such that $\Delta\phi_0=\pi/2$, we have in the limit of small phase shifts (small magnetic fields)

$$\langle\hat{j}\rangle=n_{\rm in}\kappa\Delta\phi_{\rm sig} . \quad (43)$$

In the second step of the calculation we determine the noise properties at the resonance point (zero magnetic field). Substituting the result for the correlation of the probe field at the output of the gas cell, Eq. (37) together with the beam-splitter relations into the nonlinear noise term

$$\langle \Delta j^2 \rangle = \left[\frac{2\epsilon_0 Ac}{\hbar\nu} \right]^2 \int_0^{t_m} \int_0^{t_m} d\tau\, d\tau' \langle \delta[E_5^{(-)}(\tau)E_5^{(+)}(\tau) - E_4^{(-)}(\tau)E_4^{(+)}(\tau)]\delta[E_5^{(-)}(\tau')E_5^{(+)}(\tau') - E_4^{(-)}(\tau')E_4^{(+)}(\tau')] \rangle , \quad (44)$$

we find after a somewhat lengthy calculation

$$\langle \Delta j^2 \rangle = \frac{3}{8\pi} N\lambda^2 L \frac{\gamma'\Gamma_c}{\overline{\Omega}_0^2} \frac{|\Omega_{\text{probe}}|^2}{\overline{\Omega}_0^2} \kappa^2 n_{\text{in}}$$
$$= \ln\left\{\frac{1}{\kappa}\right\} \frac{\gamma'}{\gamma} \frac{|\Omega_{\text{probe}}|^2}{\overline{\Omega}_0^2} \kappa^2 n_{\text{in}} . \quad (45)$$

In the second line of Eq. (45) we have substituted $\wp$ with the radiative decay rate γ and have introduced the Rabi frequency of the coherent probe field at the input of the phaseonium gas cell $\Omega_{\text{probe}} = \wp \overline{E}^{(+)}(0)/\hbar$.

For physically reasonable parameter values, the noise term (45) due to the interaction with the atomic medium can be made small compared to the shot-noise contribution

$$\langle \Delta j^2 \rangle_{\text{shot}} = \frac{1+\kappa^2}{2} n_{\text{in}} , \quad (46)$$

and the magnetometer sensitivity is purely shot-noise limited.

Equating the expressions for the measurement error, Eq. (46), with that of the signal, Eq. (43), we find the minimum detectable magnetic-field strength

$$B_{\min} = \frac{1}{a} \frac{4\pi}{3} \frac{1}{\lambda^2 LN} \frac{\overline{\Omega}_0^2}{\gamma} \left[\frac{1+\kappa^2}{2\kappa^2} \right]^{1/2} \left[\frac{\hbar\nu}{P_{\text{in}} t_m} \right]^{1/2} . \quad (47)$$

The first term in Eq. (47) decreases with increasing number density N or interaction length L. On the other hand, the transmission of the coherent atomic medium decreases as well as can be recognized from Eq. (19b), which leads to an enhancement of the second term. An optimum is reached if

$$\frac{4\pi}{3} \frac{1}{\lambda^2 LN} \frac{\overline{\Omega}_0^2}{\gamma} \approx \Gamma_c . \quad (48)$$

Under these conditions we obtain

$$B_{\min} \approx \frac{\Gamma_c}{a} \left[\frac{\hbar\nu}{P_{\text{in}} t_m} \right]^{1/2} , \quad (49)$$

which is the main result of this paper.

It is useful at this point to consider a numerical example. Reasonable parameters are $\gamma = 10^7\ \text{s}^{-1}$, $\Gamma_c = 10^3\ \text{s}^{-1}$, $\overline{\Omega}_0 = \gamma$, $\lambda = 500$ nm, $L = 10$ cm, $t_m = 1$ s, $P_{\text{in}} = 1$ mW, $a = 10^7\ \text{s}^{-1}/\text{G}$, and $N = 2 \times 10^{12}\ \text{cm}^{-3}$ (10^{-4} Torr at room temperature). In order to stay within the linear approximation of the probe-field interaction, the Rabi frequency of the probe field Ω_{probe} needs to be smaller than γ and hence $A \geq 1\ \text{cm}^2$. The minimum detectable field for this case is of the order of 10^{-12} G. To compare this value of the sensitivity with that of "state-of-the-art" SQUID's, we have to consider the minimum magnetic energy E_{mag} detectable with the optical magnetometer. Folding the probe laser several times back and fourth through the coherent medium, we can operate with a small sample volume. In an interaction volume of 1 cm^3 we obtain for $E_{\text{mag}} t_m$ the theoretical value of $\sim 4 \times 10^{-33}$ J s, which is of the same order as that of state-of-the-art SQUID's.

IV. INFLUENCE OF DOPPLER BROADENING

In the preceding sections we have assumed that both the driving and the test field are in resonance with the corresponding transitions if there is no magnetic field. We therefore implicitly assumed that there is no inhomogeneous broadening. In this section we study the influence of Doppler broadening on the magnetometer signal and will derive conditions under which Doppler broadening can be essentially eliminated.

The width of the susceptibility spectrum in Fig. 2 is of the order of a few natural linewidths of the optical transition. Therefore one might expect that an atomic velocity distribution and the associated Doppler shifts wash out the dip in the absorption spectrum and the large dispersion at the resonance point. We will show, however, that for approximately equal frequencies of the $a \to b$ and the $a \to c$ transition Doppler broadening can be eliminated if the probe and driving field have the same propagation direction. The physical reason for this behavior is the two-photon nature of the process.

To demonstrate the elimination of the Doppler effect we concentrate on a subgroup of atoms with a velocity component v in the z direction. In this case the detunings of the probe and driving field, Δ and Δ', Eq. (18), get an additional component

$$\Delta = \frac{\mu_B}{\hbar} g_b B + \omega_{ab} \frac{v}{c} , \quad (50)$$

$$\Delta' = -\frac{\mu_B}{\hbar} g_c B + \omega_{ac} \frac{v}{c} . \quad (51)$$

From the expression for the polarization of the probe-field transition, Eq. (14c), we recognize that it is essentially the difference of the two detunings which determines the atomic polarization. In particular we see that the denominator of Eq. (14c) becomes independent on the atomic velocity distribution if

$$r\Delta_D^2 \ll \overline{\Omega}_0^2 , \quad r\Delta_D(\gamma+\gamma') \ll 2\overline{\Omega}_0^2 , \quad \Gamma_c \Delta_D \ll 2\overline{\Omega}_0^2 , \quad (52)$$

where Δ_D is the Doppler width of the optical transition and $r = (\omega_{ab} - \omega_{ac})/\omega_{ab}$. When the frequencies of the probe and driving transition become very close and $\overline{\Omega}_0$ is sufficiently large, these relations are practically always fulfilled. If the levels b and c are, for example, hyperfine levels of the ground state in alkalines, r is of order 10^{-6}, so that for a Doppler width of $10^9\ \text{s}^{-1}$, already a Rabi frequency of $10^7\ \text{s}^{-1}$ would be sufficient to fulfill (52). Under conditions (52) the contribution of the considered atomic velocity group to the real and imaginary part of the macroscopic susceptibility near resonance are

$$\chi'_v \approx -\frac{p^2 N_v}{\hbar\epsilon_0}\frac{\left[aB+\frac{v}{c}\omega_{cb}\right]}{\overline{\Omega}_0^2}, \tag{53a}$$

$$\chi''_v \approx \frac{\wp^2 N_v}{\hbar\epsilon_0}\left[\frac{\Gamma_c}{2}\left[\overline{\Omega}_0^2-\omega_{ab}\omega_{cb}\frac{v^2}{c^2}\right] + \frac{(\gamma+\gamma')}{2}\omega_{cb}^2\frac{v^2}{c^2}\right]\frac{1}{\overline{\Omega}_0^4}. \tag{53b}$$

After averaging over the velocity distribution, the second term in Eq. (53a) disappears, since it is linear in v. That means Doppler broadening does not affect the dispersion of the material at the operating point and therefore does not affect the phase shift of the probe field. The absorption of the material can, however, be influenced by the Doppler effect. We find for the transmittivity κ of the phaseonium gas

$$\kappa=\exp\left\{-\frac{3}{8\pi}\lambda^2 LN\frac{\gamma}{\overline{\Omega}_0^2}\left[\Gamma_c+(\gamma+\gamma')r^2\frac{\Delta_D^2}{\overline{\Omega}_0^2}\right]\right\}. \tag{54}$$

For the above-mentioned example of hyperfine levels in alkalines, even the effect on the transmittivity is negligible. Thus we have shown that the magnetometer can operate essentially Doppler free if the probe and driving field frequencies differ only slightly and the Rabi frequency of the driving field is sufficiently large, such that conditions (52) are fulfilled.

V. COLLISIONAL PUMPING INTO LEVEL c

If levels b and c are closely spaced, as it should be the case in order to cancel Doppler broadening, the energy spacing $\hbar\omega_{bc}$ might be less than the thermal energy $k_B T$. In this case thermal processes drive population back and forth between levels c and b with a rate R. In a dilute gas this rate is determined essentially by the time between successive collisions with the walls of the gas cell or other atoms and is small. Nevertheless the nonzero population in level c leads to spontaneous emission noise on the a-b transition and hence to an enhancement of the total measurement error. In this section we discuss the influence of collisional pumping on the susceptibility of the medium and calculate the noise contribution in lowest order of both the pump rate R and the probe field.

In the case of a pump process from b to c with rate R, we have to modify the equations of motion (11) and (12)

$$\langle \dot{\hat\sigma}_a^{(0)}\rangle = -(\gamma+\gamma')\langle\hat\sigma_a^{(0)}\rangle - i\overline{\Omega}_0(\langle\sigma_{20}^{(0)}\rangle - \text{c.c.}), \tag{55a}$$

$$\langle \dot{\hat\sigma}_b^{(0)}\rangle = R(\langle\hat\sigma_c^{(0)}\rangle - \langle\hat\sigma_b^{(0)}\rangle) + \gamma\langle\hat\sigma_a^{(0)}\rangle, \tag{55b}$$

$$\langle \dot{\hat\sigma}_{20}^{(0)}\rangle = -[i\Delta'+\tfrac{1}{2}(\Gamma+R)]\langle\hat\sigma_{20}^{(0)}\rangle + i\overline{\Omega}_0(\langle\hat\sigma_c^{(0)}\rangle - \langle\hat\sigma_a^{(0)}\rangle), \tag{55c}$$

$$\langle \dot{\hat\sigma}_0^{(1)}\rangle = -[i\Delta+\tfrac{1}{2}(\gamma+\gamma'+R)]\langle\hat\sigma_0^{(1)}\rangle + i\frac{\wp}{\hbar}\overline{E}^{(+)}(\langle\hat\sigma_b^{(0)}\rangle - \langle\hat\sigma_a^{(0)}\rangle) + i\overline{\Omega}_0\langle\hat\sigma_{10}^{(1)}\rangle, \tag{55d}$$

$$\langle \dot{\hat\sigma}_{10}^{(1)}\rangle = -[i(\Delta-\Delta')+\tfrac{1}{2}\Gamma_c+R]\langle\hat\sigma_{10}^{(1)}\rangle - i\frac{\wp}{\hbar}\overline{E}^{(+)}\langle\hat\sigma_{20}^{\dagger(0)}\rangle + i\overline{\Omega}_0\langle\hat\sigma_0^{(1)}\rangle. \tag{55e}$$

For sufficiently small R, i.e., $R \ll \gamma$, we find near resonance under the conditions used in Sec. II

$$\langle\hat\sigma_c^{(0)}\rangle \approx \langle\hat\sigma_a^{(0)}\rangle \approx \frac{R}{\gamma}, \tag{56a}$$

$$\langle\hat\sigma_{20}^{(0)}\rangle \approx 0, \tag{56b}$$

and

$$\langle\hat\sigma_0^{(1)}\rangle \approx i\frac{\wp}{\hbar}\overline{E}^{(+)}\frac{i(\Delta-\Delta')+(\frac{1}{2}\Gamma_c+R)}{\overline{\Omega}_0^2}. \tag{56c}$$

From this result we recognize that a small thermal pump into level c does not change the index of refraction. It, however, enhances the absorption. The transmittivity of the medium now reads

$$\kappa=\exp\left\{-\frac{3}{8\pi}\lambda^2 LN\frac{\gamma}{\overline{\Omega}_0^2}\left[(\Gamma_c+2R)+(\gamma+\gamma')r^2\frac{\Delta_D^2}{\overline{\Omega}_0^2}\right]\right\}. \tag{57}$$

The enhancement of the absorption due to a small pump into the upper level is on the first glance somewhat counterintuitive. It can be understood, however, if one recognizes that the pump process does not only increase the population in the upper level, but also destroys coherence on the b-c transition. For small pump rates the second effect supersedes the first one, and the absorption is therefore enhanced.

To calculate the noise contribution we note that in the presence of the pump rate R, there are contributions to the effective noise operator $\mathcal{F}_p$ already in zeroth order of the probe field. They result from the zeroth-order contributions in the diffusion coefficients of $\mathcal{F}_{\sigma_0}$ and $\mathcal{F}_{\sigma_{10}}$, which read

$$\begin{aligned}\langle\mathcal{F}_{\sigma_0}^*\mathcal{F}_{\sigma 0}\rangle^{(0)} &= R\langle\sigma_a{}^{(0)}\rangle \approx \frac{R^2}{\gamma},\\ \langle\mathcal{F}_{\sigma_{10}}^*\mathcal{F}_{\sigma_{10}}\rangle^{(0)} &= R(\langle\sigma_b^{(0)}\rangle + \langle\sigma_c^{(0)}\rangle) + \gamma'\langle\sigma_a^{(0)}\rangle + \tfrac{1}{2}\Gamma_c\langle\sigma_c^{(0)}\rangle \approx R\frac{\gamma+\gamma'}{\gamma}.\end{aligned} \tag{58}$$

Taking into account only these contributions, we find for the effective noise operator

$$\mathcal{F}_p = \frac{1}{\overline{\Omega}_0^2}\left[\frac{\Gamma_c}{2}\mathcal{F}_{\sigma_0} + i\overline{\Omega}_0\mathcal{F}_{\sigma_{10}}\right], \tag{59}$$

and thus for the effective diffusion coefficient

$$\langle\mathcal{F}_p^*\mathcal{F}_p\rangle \approx \frac{R(\gamma+\gamma')}{\gamma\overline{\Omega}_0^2}. \tag{60}$$

Following the procedure in Sec. III we find from Eq. (60) a contribution to the measurement error

$$\langle \Delta j^2 \rangle_{\text{pump}} = \frac{3}{4\pi} N \lambda^2 L \frac{R(\gamma+\gamma')}{\overline{\Omega}_0^2} \frac{(1-\kappa^2)}{\ln(1/\kappa^2)} n_{\text{in}} , \quad (61)$$

which under optimum conditions, Eq. (48), is approximately

$$\langle \Delta j^2 \rangle_{\text{pump}} \approx \frac{R}{\Gamma_c} \frac{\gamma+\gamma'}{\gamma} \langle \Delta j^2 \rangle_{\text{shot}} . \quad (62)$$

Since $R \le \gamma_c$ and usually the linewidth of the driving laser γ_L is larger than the collisional decay rate in a coated cell, we may neglect the noise contribution due to collisional pumping into level c.

VI. COMPARISON TO OPTICAL PUMPING MAGNETOMETER

The detection of magnetic fields via optical pumping techniques was first described by Franken and Colegrove in helium [16] and improved by Cohen-Tannoudji *et al.* [17] and Kastler [18] and others. An atomic system with three lower magnetic sublevels, say $m_J = +1, 0, -1$ and one upper level, is driven by resonant unpolarized light. A magnetic field, which for simplicity we take to be parallel to the propagation direction, splits the energies by an amount $\hbar a B$. Due to optical pumping, the population of the $m_J = \pm 1$ states is driven into the $m_J = 0$ level and the pump light will be transmitted through the otherwise absorbing gas.

Now, if there is a rf signal applied to the gas which is resonant to the sublevel transition, the atoms will be driven back to the $m_J = \pm 1$ states and the gas will again absorb the optical radiation. Thus by monitoring the transmitted pumping light while varying the rf one has a sensitive measure of the spacing of the magnetic sublevels. This is summarized in Fig. 5. The ultimate precision to which we can measure this frequency and the strength of the magnetic field is determined by the intensity fluctuations Δm of the transmitted light. To measure the resonance frequency, one determines the positions of the half maxima. The intensity fluctuations at these points lead to an error $\Delta\omega_{\text{error}} = |\partial\omega/\partial m| \Delta m$, where $\partial m/\partial\omega$ is the slope of the transmission curve at the half maximum. Assuming that the intensity fluctuations are only due to shot noise we find for the frequency error under optimum conditions

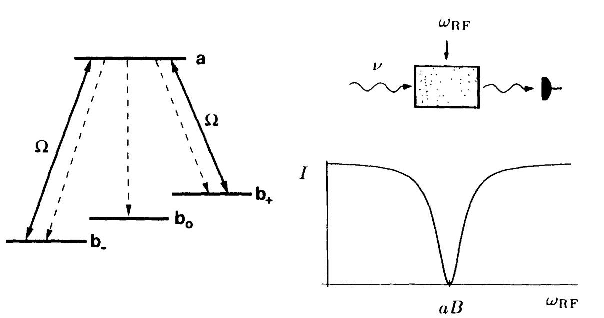

FIG. 5. Optical-pumping magnetometer: atomic level scheme and principle of operation. Optical field dumps population into levels b_0 and renders the medium transparent. The resonant rf field drives population back and leads to absorption of the optical field. Magnetic-field strength is detected by monitoring transmitted light intensity as function of rf frequency.

$$\Delta\omega_{\text{error}} = \gamma_{\text{mag}} \left[\frac{\hbar\nu}{P_{\text{in}} t_m} \right]^{1/2} , \quad (63)$$

where P_{in} is again the input power, ν is the frequency of the pump field, and t_m is the measurement time. γ_{mag} is the width of the transmission line, which in the absence of power broadening is the transverse decay rate γ_c of the rf transition. Equating the signal frequency to the error we arrive at the minimum detectable magnetic field for the optical pumping magnetometer

$$B_{\min} = \frac{\gamma_{\text{mag}}}{a} \left[\frac{\hbar\nu}{P_{\text{in}} t_m} \right]^{1/2} . \quad (64)$$

For small input powers, where $\gamma_{\text{mag}} \sim \gamma_c$, the optical pumping magnetometer gives the same sensitivity as the phaseonium magnetometer. (Note that we have ignored other noise sources than shot noise.) However, as P_{in} grows, the transmission line gets power broadened and γ_{mag} increases. In order to see the effect on the magnetometer sensitivity, we calculate the width of the transmission line by solving the corresponding density-matrix equations within a second-order perturbation approach in the rf field. We thereby consider the level configuration shown in Fig. 5.

In the interaction picture we have the equations of motion for the populations

$$\dot\rho_{b_+b_+} = \gamma_+ \rho_{aa} + i(\Omega^* \rho_{ab_+} - \text{c.c.}) - i(\Omega_{\text{rf}}^* \rho_{b_+b_0} - \text{c.c.}) , \quad (65a)$$

$$\dot\rho_{b_0b_0} = \gamma_0 \rho_{aa} + i(\Omega_{\text{rf}}^* \rho_{b_+b_0} - \text{c.c.}) - i(\Omega_{\text{rf}}^* \rho_{b_0b_-} - \text{c.c.}) , \quad (65b)$$

$$\dot\rho_{b_-b_-} = \gamma_- \rho_{aa} + i(\Omega^* \rho_{ab_-} - \text{c.c.}) + i(\Omega_{\text{rf}}^* \rho_{b_0b_-} - \text{c.c.}) , \quad (65c)$$

for the rf polarizations

$$\dot\rho_{b_+b_0} = -(i\Delta+\gamma_c)\rho_{b_+b_0} - i\Omega_{\text{rf}}(\rho_{b_+b_+} - \rho_{b_0b_0}) + i\Omega^* \rho_{ab_0} , \quad (66a)$$

$$\dot\rho_{b_0b_-} = -(i\Delta+\gamma_c)\rho_{b_0b_-} - i\Omega_{\text{rf}}(\rho_{b_0b_0} - \rho_{b_-b_-}) - i\Omega \rho_{ab_0}^* , \quad (66b)$$

and for the optical polarization

$$\dot\rho_{ab_0} = -\frac{\Gamma}{2}\rho_{ab_0} - i\Omega_{\text{rf}}^* \rho_{ab_-} - i\Omega_{\text{rf}} \rho_{ab_+} + i\Omega \rho_{b_+b_0} + i\Omega \rho_{b_-b_0} . \quad (67)$$

Here $\gamma_+, \gamma_-, \gamma_0$ are the longitudinal decay rates of the optical transitions, $\Gamma = \gamma_+ + \gamma_- + \gamma_0$, Ω_{rf} and Ω are the

Rabi frequencies of the rf and optical field, and Δ is the detuning of the rf from the magnetic transition frequency. In the absence of the rf field all population is optically pumped into level b_0 and the medium is totally transparent with respect to the optical field. With the rf coupling, population is driven back into levels $|b_\pm\rangle$ and the optical field is absorbed. The absorption is given by the imaginary part of the optical susceptibility, for which we find from Eqs. (65)–(67)

$$\chi''=\frac{\wp^2 N}{\hbar\epsilon_0}\frac{\Omega_{\rm rf}^2}{\Delta^2+\gamma_c^2+\dfrac{4|\Omega|^2\gamma_c}{\Gamma}}\left[\gamma_c+\frac{2|\Omega|^2}{\Gamma}\right] . \quad (68)$$

As can be seen, an increasing Rabi frequency Ω leads to a power broadened transmission line with width

$$\gamma_{\rm mag}=\gamma_c\left[1+\frac{4|\Omega|^2}{\gamma_c\Gamma}\right]^{1/2} . \quad (69)$$

For a sufficiently small input power, such that $\gamma_{\rm mag}\approx\gamma_c$, the minimum detectable magnetic field, Eq. (64), decreases with increasing input power $P_{\rm in}$. However, above a certain value $P_{\rm in}^c$, corresponding to the critical value of the optical Rabi frequency $\Omega^c=\sqrt{\gamma_c\Gamma/4}$, $B_{\rm min}$ saturates and approaches the value $B_{\rm min}\rightarrow(1/a)\sqrt{\gamma_c/t_m}\sqrt{3\lambda^2/2\pi A}$, where A is the pump laser cross section. In Fig. 6 we have plotted the sensitivity of the phaseonium magnetometer and the optical pumping magnetometer for the same set of parameters as a function of the laser power. One can see that the phaseonium magnetometer gives much higher sensitivities because it does not suffer from power broadening. It should be noted that the value of the probe-field Rabi frequency in the phaseonium magnetometer must be considerably smaller than the driving-field Rabi frequency in order to satisfy linearity. This, however, gives a much larger upper bound for $\Omega_{\rm probe}$ as compared to the optical pumping case. It should be noted, furthermore, that we have disregarded atomic noise in the discussion of the optical pumping magnetometer, which can significantly contribute to the measurement error.

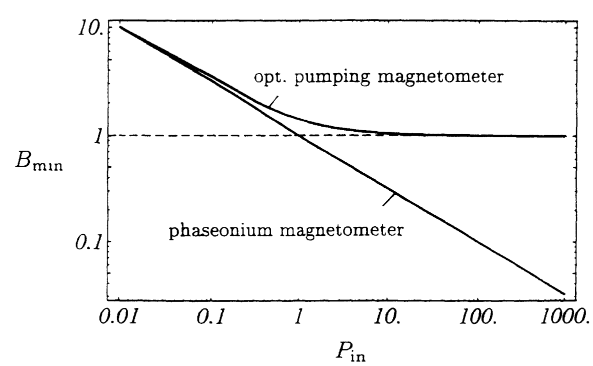

FIG. 6. Sensitivity of optical pumping and phaseonium magnetometer, as a function of laser power in units of the critical power $P_{\rm in}^c$.

VII. SUMMARY

In this article we have analyzed the quantum noise limits of the sensitivity of an optical magnetometer based on atomic phase coherence. The high dispersion of a phaseonium gas at the point of zero absorption is used to detect small magnetic level shifts via the change of the index of refraction. If we put the phase coherent material in one arm of a Mach-Zehnder interferometer, the optical phase shift associated with this variation of the refractive index can be measured with very high accuracy.

It was shown that the magnetometer is basically shot-noise limited and does not suffer from power broadening, which is the reason for the enhanced sensitivity of the device when compared to the standard optical pumping magnetometer. Because of the coherent cancellation of absorption, noise contributions from the interaction of the probe field with the medium are small. Using a balanced measuring technique additional intensity fluctuations of the input probe field are eliminated. The effect of Doppler broadening is mitigated if the transition frequencies of the pump and probe field are close (such as in the case of hyperfine sublevels) and both fields propagate in the same direction.

Another advantage of the proposed magnetometer is its large dynamical range of operation. In conventional optical magnetometer high sensitivity is achieved only when additional laboratory fields are shielded. For the phaseonium magnetometer the dynamical range is basically limited by the width of the transmission dip in the susceptibility spectrum of the material. For the parameters used in the above example this is of order 10^7 s^{-1}, corresponding to dynamical range of at least 0.1 G.

In conclusion, we emphasize that the optical phaseonium magnetometer is an interesting alternative to a SQUID. The principle sensitivity limits are comparable or even superior to the actual sensitivity of state-of-the-art SQUID's, but can be achieved without the need of cryogenic cooling and in a large dynamical range.

ACKNOWLEDGMENTS

This work was supported by the Office of Naval Research. The authors wish to thank E. Fry, D. Colegrove, M. Fink, S. Kanorsky, J. Keto, S. DiMarco, H. Pilloff, H. Walther, A. Weis, J. Wikswo, and Shi-Yao Zhu for stimulating discussions.

APPENDIX A

1. Quantum diffusion coefficients

The operator Langevin Eqs. (5) have the structure

$$\dot{\hat{x}}(t)=\hat{A}_x(t)+\hat{F}_x(t) , \quad (A1)$$

where $\hat{A}_x$ is the deterministic part of the equation and $\hat{F}_x$ is the quantum noise operator. The associated diffusion coefficients can be calculated using the generalized dissipation-fluctuation theorem [10,12]

$$\langle\hat{F}_x\hat{F}_y\rangle=-\langle\hat{x}\hat{A}_y\rangle-\langle\hat{A}_x\hat{y}\rangle+\frac{d}{dt}\langle\hat{x}\hat{y}\rangle . \quad (A2)$$

From this we obtain

$$\langle \hat{F}_a \hat{F}_a \rangle = (\gamma + \gamma') \langle \hat{\sigma}_a \rangle , \tag{A3}$$

$$\langle \hat{F}_b \hat{F}_b \rangle = \gamma \langle \hat{\sigma}_a \rangle , \tag{A4}$$

$$\langle \hat{F}_a \hat{F}_b \rangle = -\gamma \langle \hat{\sigma}_a \rangle , \tag{A5}$$

$$\langle \hat{F}_b \hat{F}_{\sigma_2} \rangle = -\gamma_c \langle \hat{\sigma}_2 \rangle , \tag{A6}$$

$$\langle \hat{F}^\dagger_{\sigma_1} \hat{F}_{\sigma_1} \rangle = \gamma' \langle \hat{\sigma}_a \rangle + \gamma_c \langle \hat{\sigma}_c \rangle , \tag{A7}$$

$$\langle \hat{F}^\dagger_{\sigma_2} \hat{F}_{\sigma_2} \rangle = \gamma_c \langle \hat{\sigma}_a \rangle , \tag{A8}$$

$$\langle \hat{F}_{\sigma_1} \hat{F}_{\sigma_2} \rangle = \gamma_c \langle \hat{\sigma}_0 \rangle . \tag{A9}$$

All other diffusion coefficients follow from (A3)–(A9) or are zero.

2. c-number diffusion coefficients

The c-number diffusion coefficients can be obtained from the quantum diffusion coefficients (A3)–(A9) by transforming the expressions in the fluctuation-dissipation theorem (A2) into normally ordered operator products. If the operator product $\hat{x}\hat{y}$ is normally ordered, its expectation value is equal to the expectation value of the corresponding c-number product. Hence we have

$$\frac{d}{dt} \langle \hat{x}\hat{y} \rangle = \frac{d}{dt} \langle xy \rangle . \tag{A10}$$

Using again the generalized dissipation-fluctuation theorem, Eq. (A2) together with its classical counterpart, we find from Eq. (A10)

$$\langle \hat{F}_x \hat{F}_y \rangle + \langle \hat{x} \hat{A}_y \rangle + \langle \hat{A}_x \hat{y} \rangle = \langle \mathcal{F}_x \mathcal{F}_y \rangle + \langle x A_y \rangle + \langle A_x y \rangle , \tag{A11}$$

where A_x and $\mathcal{F}_x$ are the deterministic term and the fluctuation operator in the c-number Langevin equation. Thus we obtain

$$\langle \mathcal{F}_x \mathcal{F}_y \rangle = \langle \hat{F}_x \hat{F}_y \rangle + \langle \hat{x} \hat{A}_y \rangle + \langle \hat{A}_x \hat{y} \rangle - \langle x A_y \rangle - \langle A_x y \rangle . \tag{A12}$$

The right-hand side of Eq. (A12) can be expressed in terms of c-number variables by normal ordering of the operator products. Hence we finally find

$$\langle \mathcal{F}_a \mathcal{F}_a \rangle = (\gamma + \gamma') \langle \sigma_a \rangle + i (\bar{\Omega}_0 \langle \sigma^*_{20} \rangle - \text{c.c.}) + i \frac{\wp}{\hbar} (\bar{E}^{(+)} \langle \sigma^*_0 \rangle - \text{c.c.}) , \tag{A13}$$

$$\langle \mathcal{F}_b \mathcal{F}_b \rangle = \gamma \langle \sigma_a \rangle + i \frac{\wp}{\hbar} (\bar{E}^{(+)} \langle \sigma^*_0 \rangle - \text{c.c.}) , \tag{A14}$$

$$\langle \mathcal{F}_a \mathcal{F}_b \rangle = -\gamma \langle \sigma_a \rangle - i \frac{\wp}{\hbar} (\bar{E}^{(+)} \langle \sigma^*_0 \rangle - \text{c.c.}) , \tag{A15}$$

$$\langle \mathcal{F}_a \mathcal{F}_{\sigma_{10}} \rangle = i \bar{\Omega}^*_0 \langle \sigma_0 \rangle - i \frac{\wp}{\hbar} \bar{E}^{(+)} \langle \sigma^*_{20} \rangle , \tag{A16}$$

$$\langle \mathcal{F}_b \mathcal{F}_{\sigma_{20}} \rangle = -i \frac{\wp}{\hbar} \bar{E}^{(+)} \langle \sigma^*_{10} \rangle , \tag{A17}$$

$$\langle \mathcal{F}_{\sigma_0} \mathcal{F}_{\sigma_0} \rangle = -2i \frac{\wp}{\hbar} \bar{E}^{(+)} \langle \sigma_0 \rangle , \tag{A18}$$

$$\langle \mathcal{F}^*_{\sigma_{10}} \mathcal{F}_{\sigma_{10}} \rangle = \gamma' \langle \sigma_a \rangle + \Gamma_c \langle \sigma_c \rangle + i \frac{\wp}{\hbar} (\bar{E}^{(+)} \langle \sigma^*_0 \rangle - \text{c.c.}) , \tag{A19}$$

$$\langle \mathcal{F}^*_{\sigma_{20}} \mathcal{F}_{\sigma_{20}} \rangle = \Gamma_c \langle \sigma_a \rangle , \tag{A20}$$

$$\langle \mathcal{F}_{\sigma_{20}} \mathcal{F}_{\sigma_{20}} \rangle = -2i \bar{\Omega}_0 \langle \sigma_{20} \rangle , \tag{A21}$$

$$\langle \mathcal{F}_{\sigma_0} \mathcal{F}_{\sigma_{10}} \rangle = -i \frac{\wp}{\hbar} \bar{E}^{(+)} \langle \sigma_{10} \rangle , \tag{A22}$$

$$\langle \mathcal{F}_{\sigma_0} \mathcal{F}_{\sigma_{20}} \rangle = -i \bar{\Omega}_0 \langle \sigma_0 \rangle - i \frac{\wp}{\hbar} \bar{E}^{(+)} \langle \sigma_{20} \rangle , \tag{A23}$$

$$\langle \mathcal{F}_{\sigma_{10}} \mathcal{F}_{\sigma_{20}} \rangle = \Gamma_c \langle \sigma_0 \rangle + i \bar{\Omega}_0 \langle \sigma_{10} \rangle + i \frac{\wp}{\hbar} \bar{E}^{(+)} (\langle \sigma_b \rangle - \langle \sigma_c \rangle) . \tag{A24}$$

All other coefficients follow from (A13)–(A24) or are zero.

APPENDIX B

1. Propagation of the driving field

In the discussion of Sec. II we have assumed a constant driving field. To verify this assumption we here discuss the susceptibility of the coherent medium with respect to the strong pump field and show that the pump field changes only very slightly while propagating through the atomic sample. The susceptibility for the pump field is determined by the a-c polarization $\langle \hat{\sigma}_2 \rangle$. The first nonvanishing term of $\langle \hat{\sigma}_2 \rangle$ is in second order of the probe field. From Eq. (5) we find

$$\langle \hat{\sigma}^{(2)}_2 \rangle \approx i \bar{\Omega} \frac{|\bar{\Omega}_{\text{probe}}|^2}{\bar{\Omega}^2_0} \frac{\frac{1}{4}\Gamma_c \frac{\gamma'}{\gamma} - i(\Delta - \Delta')}{\bar{\Omega}^2_0} , \tag{B1}$$

where we have assumed small detunings. From this we obtain

$$\chi'_{\text{pump}} = \frac{\wp'^2 N}{\hbar \epsilon_0} \frac{(\Delta - \Delta')}{\bar{\Omega}^2_0} \frac{|\bar{\Omega}_{\text{probe}}|^2}{\bar{\Omega}^2_0} ,$$
$$\chi''_{\text{pump}} = \frac{\wp'^2 N}{\hbar \epsilon_0} \frac{\Gamma_c}{4\bar{\Omega}^2_0} \frac{\gamma'}{\gamma} \frac{|\bar{\Omega}_{\text{probe}}|^2}{\bar{\Omega}^2_0} . \tag{B2}$$

In order to estimate the change of the pump-field amplitude and phase during the propagation through the coherent medium, we assume $\bar{\Omega}_{\text{probe}}(z) \approx \bar{\Omega}_{\text{probe}}(0)$, and note that $\gamma' \sim \gamma$. As we have seen in Sec. III an optimum operation of the magnetometer is reached if the interaction length and the atomic number density are chosen in such a way that the probe-field intensity at the end of the phaseonium gas cell is decreased by a factor $1/e$. The real part of the probe-field susceptibility is for magnetic-field strength of order 10^{-6} G—corresponding to $\Delta - \Delta' \sim 10$ s^{-1}—of order 10^{-8}. The absorption and the dispersion for the pump field essentially differ from these values by the ratio of the probe and pump Rabi frequencies squared, $|\bar{\Omega}_{\rm probe}|^2/\bar{\Omega}_0^2$, which we can recognize by comparing Eq. (B2) with Eq. (16). Since we consider here the case of a weak probe field, this ratio is small compared to unity. Therefore the influence of the medium on the pump field is negligible and we may assume an undepleted driving field.

APPENDIX C

1. Derivation of Eqs. (27) and (30)

To describe the noise properties of a field propagating through a sample of atoms we apply a technique introduced by Drummond and Carter [19]. Following this approach we subdivide the quantization length $(-ct_m/2, ct_m/2)$ in $2M+1$ intervals each of length $ct_m/2M+1$. The center points of the intervals are

$$z_n=\frac{nct_m}{2M+1}\ , \quad n=-M,\dots,M\ . \tag{C1}$$

We consider the case of a quasimonochromatic field with mean frequency ν and a corresponding wave number k. Since a description of a propagating field requires a multimode approach, we include a finite number of modes with creation and annihilation operators $c_n^\dagger$ and c_n. The corresponding wave numbers are

$$k_n=k+\frac{2n\pi}{ct_m}\ , \quad n=-M,\dots,M\ . \tag{C2}$$

The interaction operator of the probe-field modes with the coherent atoms reads

$$H^{\rm int}=-\hbar g\sum_{i,n,m}(\hat{c}_n^\dagger\hat{\sigma}_0^{m,i}e^{-i(k_n-k)z_m}+{\rm H.a.})\ . \tag{C3}$$

Here the index m characterizes the position of the atom and i is a number index. Note that for points inside the interaction region $\sum_i=(ct_m/L)\mathcal{N}/2M+1$ is the number of atoms in one length interval ($\mathcal{N}$ is the total number of atoms in the sample). The coupling constant g is related to the dipole moment $\wp$ and the quantization volume Act_m via

$$g=\frac{\wp}{\hbar}\left[\frac{\hbar\nu}{2\epsilon_0 Act_m}\right]^{1/2}. \tag{C4}$$

At this point it is convenient to introduce the new field variables

$$\hat{b}_l=\frac{1}{(2M+1)^{1/2}}\sum_{n=-M}^{M}\hat{c}_n\exp\left\{\frac{2\pi inl}{2M+1}\right\}\ , \quad l=-M,\dots,M \tag{C5}$$

which fulfill the Bose commutation relations

$$[\hat{b}_l,\hat{b}_{l'}^\dagger]=\delta_{ll'}\ . \tag{C6}$$

In terms of these field variables the total Hamiltonian can be written as

$$\begin{aligned}H&=H_{\rm atom}^0+\sum_n\hbar\nu_n\hat{c}_n^\dagger\hat{c}_n+H^{\rm int}\\&=H_{\rm atom}^0+\hbar\nu\sum_l\hat{b}_l^\dagger\hat{b}_l+\hbar\sum_{\substack{l,l'\\l\neq l'}}\nu_{ll'}\hat{b}_l^\dagger\hat{b}_{l'}\\&\quad-\hbar g\sum_{i,l}\{(2M+1)^{1/2}\hat{b}_l^\dagger\hat{\sigma}_0^{i,l}+{\rm H.a.}\}\ .\end{aligned} \tag{C7}$$

Here the last sum is taken only over l values corresponding to positions inside the interaction region and

$$\nu_{ll'}=\sum_{n=-M}^{M}\frac{2\pi nc}{(2M+1)ct_m}\exp\left\{\frac{2\pi in(l-l')}{2M+1}\right\}. \tag{C8}$$

From Eq. (C7) we find the equation of motion of the slowly varying field amplitude

$$\dot{\hat{b}}_l=-i\sum_{l'}\nu_{ll'}\hat{b}_{l'}+ig\sum_i(2M+1)^{1/2}\hat{\sigma}_0^{i,l}\ . \tag{C9}$$

We proceed by transforming into c numbers and apply a continuous approximation in the limit $M\to\infty$. In this limit we have the following correspondences:

$$\begin{aligned}&\frac{lct_m}{2M+1}\to z\ ,\\&(2M+1)^{1/2}b_l\to\alpha(z,t)\ ,\\&-i\sum_{l'}\nu_{ll'}b_{l'}(2M+1)^{1/2}\to-c\frac{\partial}{\partial z}\alpha(z,t)\ .\end{aligned} \tag{C10}$$

Thus the equation of motion for the space- and time-dependent complex amplitude of the probe field reads

$$\left[\frac{\partial}{\partial t}+c\frac{\partial}{\partial z}\right]\alpha(z,t)=ig\lim_{M\to\infty}(2M+1)\sum_i\sigma_0^{i,l}\Big|_{z_l\to z}\ . \tag{C11}$$

Making use of the relation between α and the field strength $E^{(+)}$

$$E^{(+)}(z,t)=\left[\frac{\hbar\nu}{2\epsilon_0 Act_m}\right]^{1/2}\cdot\alpha(z,t)\ , \tag{C12}$$

we obtain from (C11)

$$\left[\frac{\partial}{\partial t}+c\frac{\partial}{\partial z}\right]E^{(+)}(z,t)=i\frac{\nu}{2\epsilon_0}P(z,t)\ , \tag{C13}$$

where we have introduced the macroscopic polarization

$$\begin{aligned}P(z,t)&=\frac{\wp}{Act_m}\lim_{M\to\infty}(2M+1)\sum_i\sigma_0^{il}\Big|_{z_l\to z}\\&=\bar{P}(z,t)+\mathcal{F}_P(z,t)\ .\end{aligned} \tag{C14}$$

The semiclassical value of P—indicated by the overbar—is given by the semiclassical value of the atomic polarization $\bar{\sigma}_0$,

$$\bar{P}(z,t)=\wp N\bar{\sigma}_0(t)|_{E=\bar{E}(z)}\ . \tag{C15}$$

$\mathcal{F}_P(z,t)$ in Eq. (C14) is a δ-correlated noise operator, which is related to the corresponding microscopic noise operator

$$\sigma_0^{il}(t)=\bar{\sigma}_0^{il}+\mathcal{F}_p^{il}(t)\ , \tag{C16a}$$

$$\mathcal{F}_P(z,t)=\frac{\wp}{Act_m}\lim_{M\to\infty}(2M+1)\sum_i \mathcal{F}_p^{il}(t)\Big|_{z_l\to z}\ . \tag{C16b}$$

Therefore we have

$$\begin{aligned}\langle \mathcal{F}_P^{(*)}(z,t)\mathcal{F}_P(z',t')\rangle &= \lim_{M\to\infty}(2M+1)^2\frac{\wp^2}{A^2c^2t_m^2}\\ &\quad\times\sum_{ij}\langle \mathcal{F}_p^{il(*)}(t)\mathcal{F}_p^{jl'}(t')\rangle\Big|_{z_l\to z, z_{l'}\to z'}\\ &=\frac{\wp^2}{A}N\langle \mathcal{F}_p^{(*)}\mathcal{F}_p\rangle\delta(t-t')\delta(z-z')\ ,\end{aligned} \tag{C17}$$

where we have used the correspondence $\lim_{M\to\infty}[(2M+1)/ct_m]\delta_{ll'}\to\delta(z-z')$.

APPENDIX D

1. Vacuum-noise contribution

In order to determine the vacuum-noise term in Eq. (40), we replace the phaseonium gas by a passive medium with transmittivity κ and solve for the quantum expression of the output signal $\hat{j}$. Denoting the field annihilation operators at the different points of the interferometer by $a_v, a_0, \ldots, a_5$ in analogy to Fig. 4, we find

$$\hat{j}=\frac{1}{t_m}\int_0^{t_m}d\tau(a_5^\dagger a_5-a_4^\dagger a_4)\ . \tag{D1}$$

Using the beam-splitter relations (38) and (39) and noting that [20]

$$a_3=\kappa e^{i\Delta\phi_{\rm sig}}a_1+\sqrt{1-\kappa^2}a_v'\ , \tag{D2}$$

where a_v' is an additional vacuum field that couples in due to the medium losses described by κ, we obtain

$$\begin{aligned}\hat{j}&=\tfrac{1}{2}(\epsilon^*+\epsilon)a_0^\dagger a_0+\frac{i}{2}\epsilon^*(a_0^\dagger a_v+a_v^\dagger a_0)\\ &\quad+\frac{i}{\sqrt{2}}\epsilon'^* a_v'^\dagger a_0-\frac{i}{2}\epsilon(a_0^\dagger a_v+a_v^\dagger a_0)-\frac{i}{\sqrt{2}}\epsilon' a_0^\dagger a_v'\\ &\quad+\text{pure vacuum terms}\ .\end{aligned} \tag{D3}$$

Here $\epsilon=\kappa e^{i(\Delta\phi_{\rm sig}-\Delta\phi_0)}$ and $\epsilon'=\sqrt{1-\kappa^2}$. The "pure vacuum terms" contain only normally ordered products of vacuum operators and hence give zero contributions to first- and second-order moments. Calculating $\langle\Delta\hat{j}^2\rangle=\langle\hat{j}^2\rangle-\langle\hat{j}\rangle^2$ from Eq. (D3) yields

$$\begin{aligned}\langle\Delta\hat{j}^2\rangle&=\kappa^2\cos^2(\Delta\phi_{\rm sig}-\Delta\phi_0)\langle\Delta n_{\rm in}^2\rangle+\tfrac{1}{2}(1-\kappa^2)\langle n_{\rm in}\rangle\\ &\quad+\kappa^2\sin^2(\Delta\phi_{\rm sig}-\Delta\phi_0)\langle n_{\rm in}\rangle\ .\end{aligned} \tag{D4}$$

At the operating point where $\Delta\phi_0=\pi/2$ we have

$$\cos^2(\Delta\phi_{\rm sig}-\Delta\phi_0)\approx 0\ ,\quad \sin^2(\Delta\phi_{\rm sig}-\Delta\phi_0)\approx 1\ . \tag{D5}$$

The vacuum noise contribution therefore reads

$$\langle\Delta\hat{j}^2\rangle=\frac{(1+\kappa^2)}{2}\langle n_{\rm in}\rangle\ . \tag{D6}$$

[1] See, for example, J. Clarke, Phys. Today **39** (3), 36 (1986).

[2] M. O. Scully and M. Fleischhauer, Phys. Rev. Lett. **69**, 1360 (1992).

[3] See, for instance, H. G. Kuhn, *Atomic Spectra* (Academic, New York, 1969).

[4] G. Alzetta, A. Gozzini, L. Moi, and G. Orriols, Nuovo Cimento B **36**, 5 (1976); E. Arimondo and G. Orriols, Nuovo Cimento Lett. **7**, 333 (1976); G. Alzetta, L. Moi, and G. Orriols, Nuovo Cimento B **52**, 209 (1979); H. Gray, R. Whitley, and C. Stroud, Opt. Lett. **3**, 218 (1979).

[5] O. Kocharovskaya and Ya. I. Khanin, Pis'ma Zh. Eksp. Teor. Fiz. **48**, 581 (1988) [JETP Lett. **48**, 630 (1988)]; O. Kocharovskaya and P. Mandel, Phys. Rev. A **42**, 523 (1990); O. Kocharovskaya, Phys. Rep. **219**, 175 (1992).

[6] M. O. Scully, S. Zhu, and A. Gavrieliedes, Phys. Rev. Lett. **62**, 2813 (1989); M. O. Scully, S. Y. Zhu, and H. Fearn, Z. Phys. D **22**, 471 (1992); S. Y. Zhu, M. O. Scully, H. Fearn, and L. M. Narducci, *ibid.* **22**, 483 (1992); M. O. Scully, Phys. Rep. **219**, 191 (1992).

[7] S. Harris, Phys. Rev. Lett. **62**, 1022 (1989); A. Imamoğlu and S. Harris, Opt. Lett. **14**, 1344 (1989); K. J. Boller, A. Imamoğlu, and S. E. Harris, Phys. Rev. Lett. **66**, 2593, (1991); J. E. Field, K. H. Hahn, and S. E. Harris, *ibid.* **67**, 3062 (1991).

[8] A. Lyras, X. Tang, P. Lambropoulos, and J. Zhang, Phys. Rev. A **40**, 4131 (1989); S. Basile and P. Lambropoulos, Opt. Commun. **78**, 163 (1990).

[9] M. Scully, Phys. Rev. Lett. **67**, 1855 (1991); M. O. Scully and Shi-Yao Zhu, Opt. Commun. **87**, 134 (1992); M. Fleischhauer *et al.*, Phys. Rev. A **46**, 1468 (1992); U. Rathe *et al.*, *ibid.* **47**, 4994 (1993).

[10] See, for instance, M. Sargent, M. Scully, and W. Lamb, *Laser Physics* (Addison-Wesley, Reading, MA, 1974).

[11] B. J. Dalton and P. L. Knight, Opt. Commun. **42**, 411 (1982).

[12] W. H. Louisell, *Quantum Statistical Properties of Radiation* (Wiley, New York, 1973).

[13] C. W. Gardiner, *Handbook of Stochastic Methods* (Springer, Berlin, 1983).

[14] C. M. Caves, Phys. Rev. D **23**, 1693 (1981).

[15] Min Xiao, Ling-An Wu, and H. J. Kimble, Phys. Rev. Lett. **59**, 278 (1987).

[16] P. A. Franken and F. D. Colegrove, Phys. Rev. Lett. **1**, 316 (1958).

[17] One of the most sensitive magnetic-field measurements with an optical-pumping magnetometer is described by C. Cohen-Tannoudji, J. DuPont-Roc, S. Haroche, and F. Laloë, Phys. Rev. Lett. **15**, 758 (1969).

[18] See A. Kastler, Nucl. Instrum. Methods **110**, 259 (1973), and references therein.

[19] P. D. Drummond and C. J. Carter, J. Opt. Soc. Am. B **4**, 1565 (1987).

[20] See, for instance, C. M. Caves, in *Quantum Optics, Experimental Gravity, and Measurement Theory,* Vol. 94 of *NATO Advanced Study Institute, Series B: Physics,* edited by P. Meystre and M. O. Scully (Plenum, New York, 1983).